

David R. Rodríguez
Florida Institute of Technology, Melbourne, FL
For the UCLA 2005 Physics REU Program

Stellar Populations Derived from Color Gradients of the Nearby Dwarf Elliptical Galaxy M32

Abstract

M32, satellite of the Andromeda Galaxy (M31), has been observed in a wide range of wavelengths from the far ultraviolet to the infrared using images from GALEX, Spitzer, HST, and Keck. The surface brightness of the galaxy is measured using an IDL procedure to fit elliptical isophotes and color gradients are obtained by comparing the surface brightness at different wavelengths. Most of the color gradients are fairly constant, with only a gradual reddening with increasing distance from the galactic center. We infer that the stellar populations must be roughly the same at all radii from the galaxy. A redder color is observed within 2 arcseconds (corresponding to about 7 parsecs) of the nucleus. STIS FUV/NUV division images show a dark area that could be dust in the central region. This dust could be responsible for the observed reddening and might come from the envelopes of AGB stars as observed in the IRAC 8 micron image. Additionally, point sources are counted for the IRAC 8 micron images. The fuel consumption theorem is applied to determine the lifetime of those stars and a value of about 27,000 or 44,000 years (depending on the method used) is obtained. This value is close to the expected lifetime of the AGB phase.

1. Introduction

M32 is a dwarf elliptical galaxy 750 kiloparsecs (about 2 million light-years) away. It is a satellite to the Andromeda Galaxy (M31) and is the nearest elliptical galaxy. It also contains a supermassive black hole of $\sim 2 \times 10^6$ solar masses (Kormendy & Richstone 1995). Because of these features, it affords us a unique opportunity to study the distribution of stellar populations in the central regions of an elliptical galaxy.

For this project, a wide range of wavelengths was used to study M32. We start from the far ultraviolet ($\sim 1400 \text{ \AA}$) and end at the infrared (~ 10 microns). In the ultraviolet images, we are seeing primarily helium burning evolved stars, such as horizontal branch stars. With the K filter, we see light from red giants and with the 8 micron images we see the circumstellar shells of asymptotic giant branch (AGB) stars. Thus, all of our images contain light from evolved stars.

Our project analyzes the surface photometry of M32 in elliptical annuli out from its center to observe how the total light falls off as a function of radius. By performing photometry at a variety of wavelengths we obtain numerous galaxy profiles that can be compared with one another. A comparison of two wavelengths yields a measure of the color of the galaxy. These color gradients will provide clues to the stellar populations present in M32 and how they change with radius.

Previous evidence has indicated that the stars present in M32 are all from the same population and that they have ages ranging from intermediate (5 Gyr) to old (10 Gyr). Rose et al. (2005) determined that near the nucleus there are younger stars ($\sim 3-4$ Gyr) with higher metallicity while older stars ($\sim 6-7$ Gyr) are located farther from the nucleus in regions of lower metallicity. Colors tend to get redder for increasing age, but

bluer for decreasing metallicity (Rose et al. 2005). Because of this, there is a net cancellation and we expect the profiles to be roughly the same at all wavelengths. This means that the color gradients should be mostly constant.

In addition to surface photometry, star counting of the brightest stars also reveals information directly about stellar populations. By counting the number of stars we can apply the fuel consumption theorem and calculate the lifetime of the observed stars in that particular phase. The individual stars we measure were best observed in the 8 micron images and as such are probably the AGB stars. These stars remain in that phase for 10 to 20 thousand years. We will infer the lifetime of the observed stars and compare it with the predicted AGB star lifetime.

Our results show a constant color with only gradual changes. This is indicative of the same stellar population throughout the galaxy. We also found an area of increased red color in the central 2 arcseconds (about 7 parsecs) of the galaxy. This redder color confirms (Worthey 2004) findings of a discontinuity in the light profile of M32 at 2 arcseconds. In addition to this, we obtain a lifetime for the stars in the 8 micron image that is within a factor of four of the expected AGB lifetime.

2. Data Sets Used

A total of six data sets were used for this project. The data come from the Galaxy Evolution Explorer (GALEX) satellite, Spitzer Space Telescope's InfraRed Array Camera (IRAC), Hubble Space Telescope's Near Infrared Camera and Multi-Object Spectrometer (NICMOS) and Space Telescope Imaging Spectrograph (STIS) instruments, Keck ground based observations, and R and K data taken from Peletier (1993). A

summary of the details on the resolution of all the instruments can be found on Table 1.

General telescope and filter information can be found in Appendix A.

2.1 GALEX

The GALEX data originally came from the MultiMission Archive at the Space Telescope Science Institute (MAST), yet in order to obtain images with higher signal to noise we used Gil de Paz's (2004) FUV and NUV images (defined in Table 1). These images are the sum of several exposures and represent 6138 seconds in FUV and 4808 in NUV. These images had to be background subtracted using the methods described in Section 3.2 in order to be able to draw the inferences presented in this paper.

Instrument	Filter	λ	$\Delta\lambda$	Field of View	Scale ("/pix)	FWHM	Exp Time
GALEX	FUV	1528 Å	1344-1786 Å	1.25deg	1.5	4.0"	6138s
GALEX	NUV	2271 Å	1771-2831 Å	1.25deg	1.5	5.6"	4808s
HST STIS	F25SRF2 FUV MAMA	1469 Å	1280-1780 Å	24.7"x24.7"	0.0247	~0.1"	13472s
HST STIS	F25Q7Z NUV MAMA	2354 Å	1460-3270 Å	24.7"x24.7"	0.0248	~0.1"	2469s
SPITZER	CH1	3.550 μ m	0.681 μ m	5.21'x5.21'	1.2	1.83"	30s
SPITZER	CH2	4.493 μ m	0.872 μ m	5.18'x5.18'	1.2	1.83"	30s
SPITZER	CH3	5.731 μ m	1.250 μ m	5.21'x5.21'	1.2	1.83"	30s
SPITZER	CH4	7.872 μ m	2.526 μ m	5.21'x5.21'	1.2	1.83"	30s
Keck	LWS 10.3	10.5 μ m	8.10-12.8 μ m	10.2"x10.2"	0.0847	0.26"	1134s
HST NICMOS	NIC2 F160W	16060 Å	1.4-1.8 μ m	19.2"x19.2"	0.0758	~0.1"	15.97s

Table 1: Instrument Summary

2.2 Spitzer

Our Spitzer images were taken with the IRAC camera described in Appendix A. In our images, M32 appears in the right half of the image for channels 1 and 3, but on the left half for channels 2 and 4. From the header files, we see that the images were taken on January 18, 2005 under program 3400, PI R. Michael Rich.

These are the first infrared images to show resolved stars around M32. Channels 1 and 2 observe the stellar photosphere at temperatures of around 4000K while channel 4 can see dust around the stars around 300K and can see PAH emissions when they glow due to UV light.

The images were cut to center on M32 and to avoid some of the high background seen in a few of the images. Channels 1 and 2 are saturated at the center of the galaxy, so measurements within 6 arcseconds are questionable.

2.3 Keck

The Keck images were taken using the Long Wavelength Spectrometer (LWS) instrument and a chop-nod cycle. The images were taken by Dr. Mark Morris and Dr. Michael Rich on October, 18 2000. A total of six images were taken of M32, each having a total exposure time of 189 seconds. The images were reduced and combined as explained in Appendix B to obtain a final clean image.

2.4 HST

Two instruments were used to gather data using the Hubble Space Telescope. These were NICMOS, which took images in the infrared, and STIS, which provided ultraviolet images. These images have small fields of view, serving as close up images of the central regions of the ultraviolet and infrared images taken by GALEX and Spitzer.

2.5 Peletier's K data

Peletier provided the surface brightness of M32 in the R band (0.65 μm) in his 1993 paper. He also provided R – K color data. The K filter lets in light of about 2.2

microns, while R is about 0.65 microns. The R data was taken using the 2.5 meter Isaac Newton Telescope. The K data was taken using the 2.1 meter Kitt Peak telescope. The K surface brightness can be obtained using: $\mu K = \mu R - (R - K)$, where μR is the surface brightness in the R band in magnitudes/arcsecond² and $R - K$ is the color data.

3. Data Analysis

Several different procedures were used to perform the different tasks that were required. The goal of this project was surface photometry of M32, yet for an accurate measure we needed to subtract the background light in each image. We also counted the point sources in the IRAC 8 μ m image in order to apply the fuel consumption theorem.

3.1 Photometry

Photometry is the measurement of the flux of an object. It determines how bright an object is. Some units of surface photometry are janskys per square arcsecond, megajanskys per steradian (MJy/sr), and magnitudes per square arcsecond. The IRAC images are already in MJy/sr while the other images are in counts or counts/second. In this project, we perform surface photometry on elliptical annuli and convert our results into magnitudes per square arcsecond.

An IDL procedure was written to perform surface photometry on M32. The procedure, **ellipse.pro**, creates an elliptical mask of ellipticity 0.28 and at an angle of -20 degrees from the y-direction. These numbers were obtained from a rough average of Peletier's surface photometry (1993). Although Peletier's axis ratio and orientation vary with radius in M32, we adopt the predominant orientation and eccentricity. In order to apply the procedure, the image is rotated so that North is up. This was done using the

IDL routines **rot** and **hrot** and reading the position angles provided on the header files. This rotated image would be passed into the procedure, which would then create the elliptical mask. After the elliptical mask was created, the mean, standard deviation, and mode of all points residing within an elliptical annulus was obtained and the process was repeated for concentric annuli. The units were then converted to the AB magnitude scale.

The conversion to the magnitude scale differed on all the images. For GALEX, the values were first divided by the area per pixel to obtain the values per arcsecond². Then, the following formula was applied (from the GALEX website¹):

$m = -2.5 \log_{10}(\text{value}) + z_0$, where z_0 is 18.82 for FUV and 20.08 for NUV. For IRAC, the images were in MJy/sr so the following was used to convert to Jansky/arcsecond²:

$S = \text{values} \times 2.35 \times 10^{-5}$. Afterwards, we used the standard AB formula:

$m = -2.5 \log_{10}(f) - 48.60$, where f is in $\text{ergs cm}^{-2} \text{ s}^{-1} \text{ Hz}^{-1}$ (Oke 1990). For NICMOS, the data handbook provides the following formula:

$m = -2.5 \log_{10}(\text{value} \times \text{PHOTFNU} \times 10^{-23}) - 48.60$, where PHOTFNU is a number

provided in the header file that converts the units into Jy and value is the measured value divided by the area per pixel. For STIS, the instrument handbook provides the following formula: $m = -2.5 \log_{10}(\text{Flux}) - 2.402 - 5.0 \log_{10}(\lambda)$, where

$\text{Flux} = \text{value} \times \text{PHOTFLAM} / \text{exposuretime}$, λ is the wavelength in Å, and value is the

measured value divided by the area of each pixel. This formula can be derived by

replacing f (in $\text{ergs cm}^{-2} \text{ s}^{-1} \text{ Hz}^{-1}$) in the standard AB formula by $f \times \lambda^2 / c$ where f is in

$\text{ergs cm}^{-2} \text{ s}^{-1} \text{ Å}^{-1}$. The Keck data was the trickiest to convert. For Keck, the formula used

¹ http://galex.stsci.edu/ero/Doc/Early_release_data_description_par2.htm

was $m = -2.5 \log_{10} \left(\frac{\text{value}}{z_0} \right) + 6$, where value is again the measured value divided by the area per pixel. The 6 at the end is to shift the data so it can be compared with NICMOS and z_0 is a calculated zero point. This zero point is obtained by taking all the light that is measured in IRAC channel 4 ($8\mu\text{m}$) in the same area as that covered in Keck. This number is then converted to counts (since IRAC images are MJy/sr) and used as the zero point. The Keck data is not properly calibrated, but what we are interested is in the color differences and not in the absolute values of surface brightness.

3.2 Background Subtraction

Three different methods were used to subtract the background sky. Most images have a relatively low and uniform background and so only one of the methods is required. For the GALEX images, the background is complex, thus making it necessary to use several methods for the most complete background subtraction.

The first method involves subtracting out the modal sky. This is the mode of values in the image and is taken to be a representation of a constant background sky. With complicated backgrounds, the deviations from a smooth background are caused by stars and nebulosity. Using the mean is incorrect since it will count these high values and pull the mean higher than the local sky. Because of this, the mode is preferred as it is a measure of the most frequent sky value. The IDL routine **MMM** in the Astronomy User's Library was used to obtain the modal sky. This function also ignores values that are not likely to be part of the sky background. The value obtained was then subtracted from the image. On the IRAC images, the modal sky was estimated on a slice of the sky that did

not contain the galaxy or any other bright features. This yielded a better estimate of the sky than what the full image would have done.

The second method involved creating a plane and subtracting it from the image. The plane was created by using a user built procedure, **plane.pro**. This procedure takes in the image and three points as input and outputs a plane based on the average value of a 3 pixel box centered on the three points. A careful selection of the three points would yield planes that subtracted the background sky near M32, although edges of the images would be greatly altered. Figure 1 shows an original FUV image and Figure 2 shows the plane subtracted image. The plane subtracted image ensures that the galaxy is located on a flat background, rather than one that has a slope. This facilitates further background subtraction.

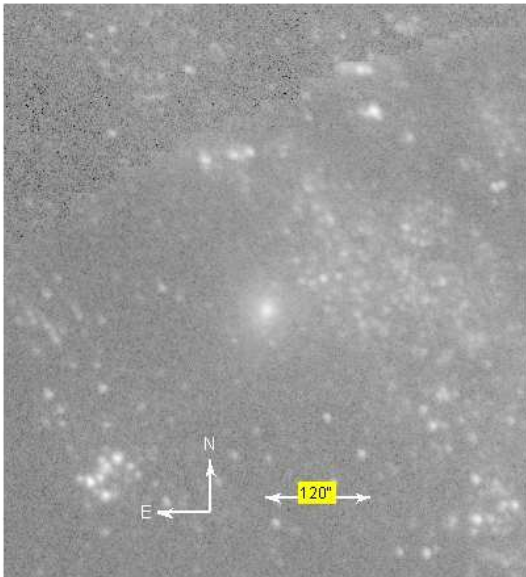


Figure 1: M32 FUV Image (GALEX)

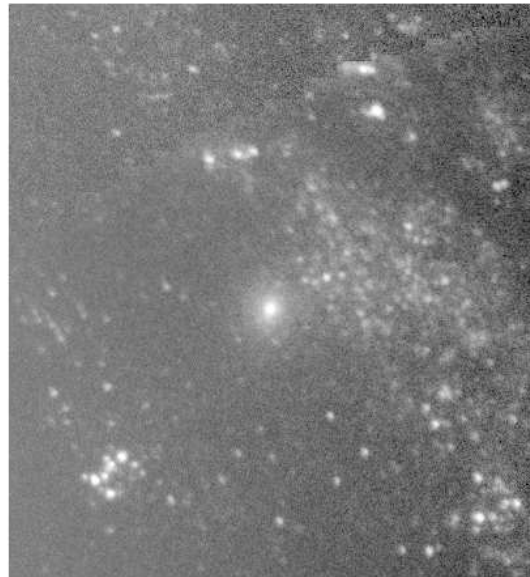


Figure 2: M32 Plane Subtracted FUV Image

The third method involved creating a model galaxy from an initial run of the photometry program, an example model for FUV GALEX is shown in Figure 3. This model galaxy could then be subtracted from the original image to obtain the background

of the image, as shown in Figure 4. This method over subtracts in the region where M32 is present, essentially creating a hole at M32's location. In order to fix this we use **MMM** to obtain the modal sky. We then set all values that are less than half the modal sky value equal to the modal sky to obtain Figure 5. This fixes the over subtraction and improves the background image. The final image to analyze would be the original image minus the background image obtained by subtracting the galaxy and setting the modal sky. This is shown in Figure 6 and it was the best image that could be obtained using our background subtraction methods. The background is not entirely subtracted, but this was the best method that could be done in our limited amount of time.

Most images only required a simple **MMM** run to get a decent sky subtraction. The GALEX images, however, required a more complicated approach, which involved applying first the second method (plane subtraction) and then the third method (galaxy subtraction).

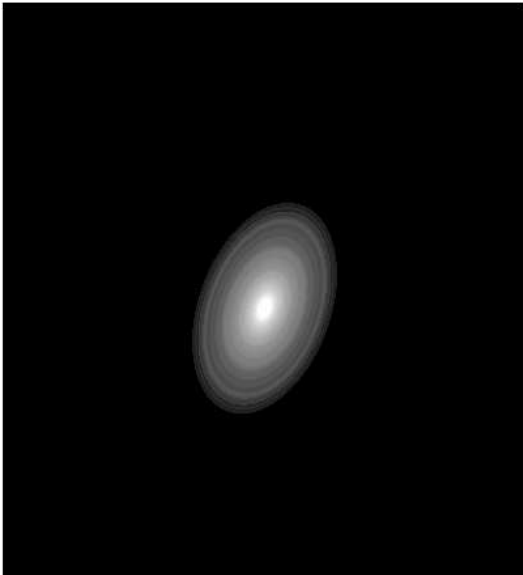


Figure 3: M32 FUV Model Galaxy

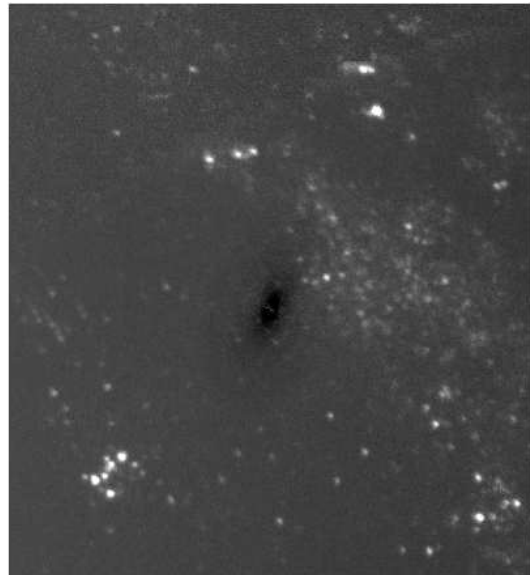


Figure 4: M32 Model galaxy subtracted from FUV image

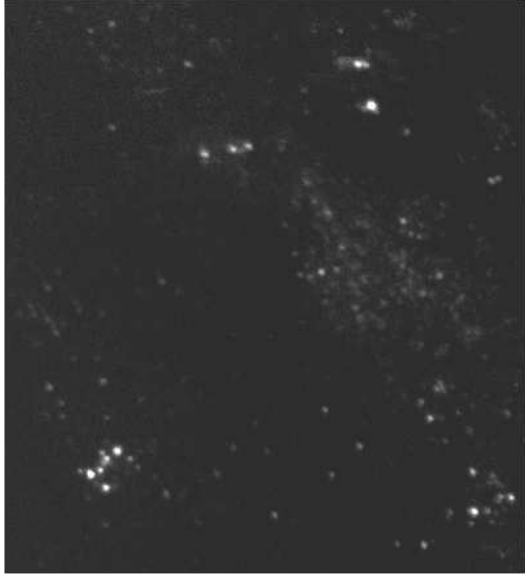


Figure 5: Modal sky subtracted background

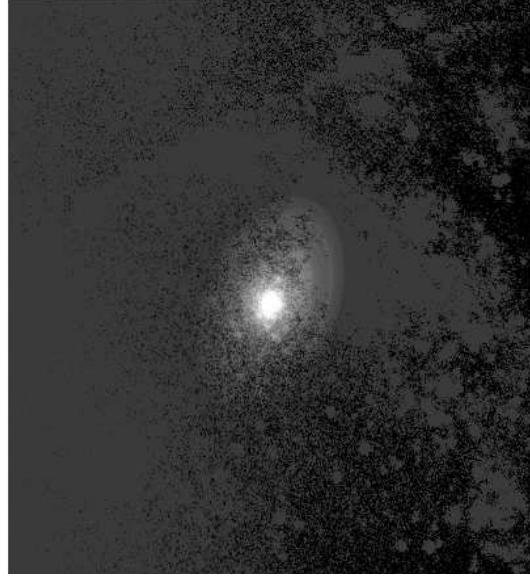


Figure 6: Final background subtracted M32 FUV image

3.3 Point Sources

Point sources were visible in the IRAC images. We decided to count and measure the resolved stars in the IRAC 8micron image. These point sources were measured by using the IDL routine **FIND** in the Astronomy User's Library. FIND will count as a point source those objects which are (1) above a threshold intensity, (2) within a certain sharpness statistic, and (3) within a certain roundness statistic. The threshold intensity was 3 sigma above background and the default values were used for sharpness (from 0.2 to 1.0) and roundness (-1.0 to 1.0). There were 183 sources found (excluding the galaxy center) and they range from about 14 to 230 arcseconds away from the center of M32. Within 14 arcseconds, we encounter the confusion limit. Within the confusion limit, individual stars cannot be resolved. The fuel consumption theorem was then applied to these stars as explained in Section 6.

4. Surface Photometry Results

We obtain surface photometry for each observed wavelength. Some of the images, however, were not properly calibrated so that the absolute surface photometry might be inaccurate. Our interest is in seeking color gradients (not absolute photometry) that may indicate changes in the stellar population, so the scale uncertainties are not a limitation.

Most of the results follow the same general trend. Figure 7 shows how the surface brightness of M32 in the FUV and NUV as a function of radius. Figure 8 shows the surface brightness for the IRAC channels and for Peletier's K data. The first few (~6) arcseconds of IRAC channels 1 and 2 show saturation. Figure 9 shows the data for HST STIS FUV and NUV. A comparison with the GALEX data is not feasible because of the resolution in GALEX. Figure 10 shows Keck and NICMOS data. The zero point of the Keck data has been shifted to force agreement with the NICMOS 8um image. Due to the small image size, the Keck data is unreliable after about 2.5 arcseconds.

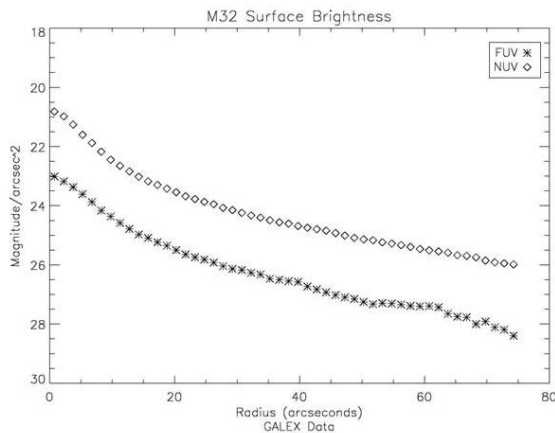


Figure 7: GALEX FUV and NUV Surface Brightness

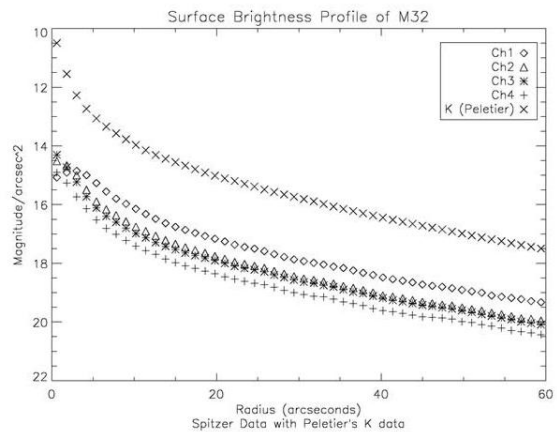


Figure 8: Spitzer and Peletier's K data

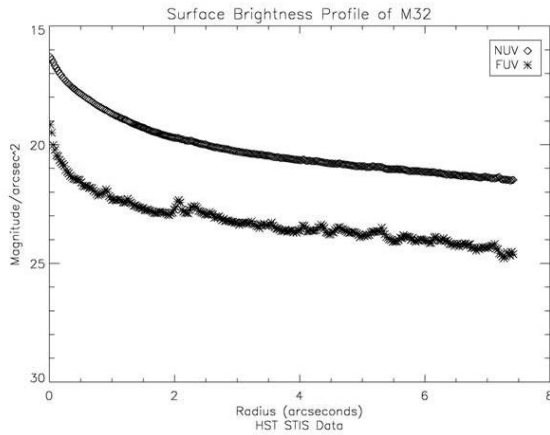


Figure 9: HST STIS data

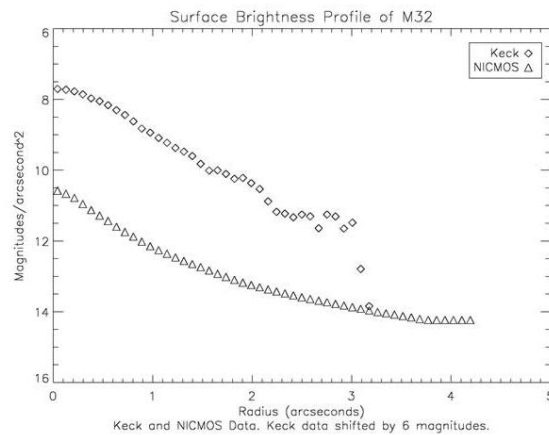


Figure 10: Keck and NICMOS data

5. Color Gradients

The color results are more consistent than the surface photometry. Most of the colors remain fairly constant with only a few exceptions. These exceptions have only a gradual color change with increasing radius.

Figure 11 shows the FUV-NUV color as a function of radius for GALEX. The data after about 50 arcseconds suffers from increasing noise and background sky. Ignoring the first 10 arcseconds we can say that the color remains fairly constant with only a gradual decrease (redder as you move out from the center). Figure 12 shows the FUV-NUV color as seen by STIS. Though there seems to be a lot of noise, it appears that the color remains fairly constant after 2 arcseconds. Within 2 arcseconds, the color gets redder by nearly one magnitude and then gets bluer by almost half a magnitude within 0.5 arcseconds. Figure 13 is an image made by dividing the SITS FUV and NUV images. There seems to be a dark area of dust in this image. This could be responsible for the redder color in the inner 2 arcseconds.

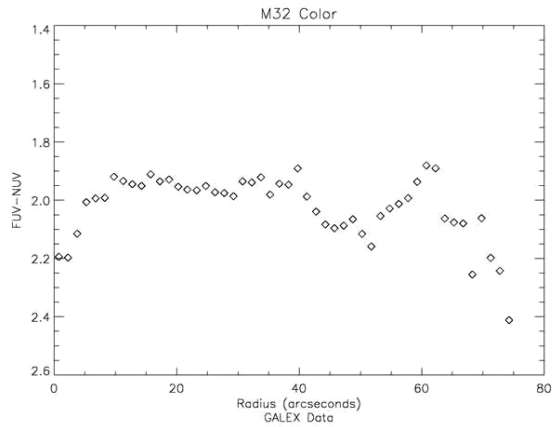


Figure 11: GALEX color data

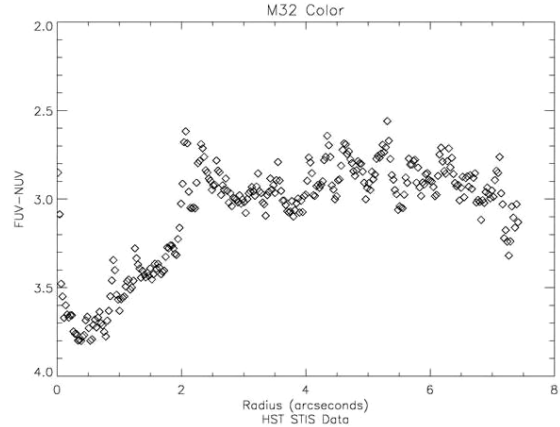


Figure 12: STIS color data

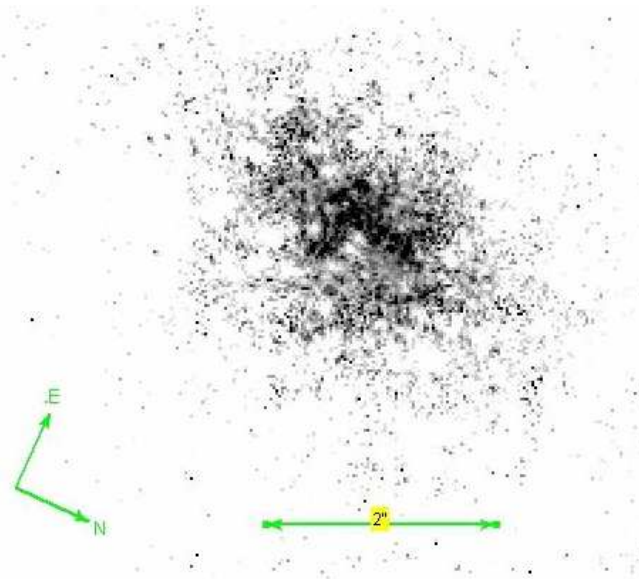


Figure 13: STIS FUV/NUV Image.

For the infrared colors, Figure 14 shows the color plot for IRAC channels 1-2 (3.6-4.5 microns) and 3-4 (5.8-8 microns). In Figure 15 and Figure 16 we see the colors for channels 1-3 and 2-4 and for 1-4 and 2-3, respectively. Every time channel 3 is compared, after 60 arcseconds, the color starts arching up (vs. channels 1 and 2) or down (vs. channel 4). This might be due to an incorrect subtraction of the sky background for that channel. The other colors change only gradually. The color for channels 1-2 becomes

slightly bluer with increasing radius, while for channels 2-4 and 1-4 the color is bluer at the galaxy center. Figure 17 shows the colors when Peletier's K data is compared with the IRAC data. The first few arcseconds show saturation, yet the general trend is for a bluer color as you move into the galaxy. The color change is gradual with less than a 0.5 magnitude change in 50 arcseconds.

In Figure 18 we see the color for GALEX FUV – IRAC Ch1 and FUV – Ch4. Both are relatively flat except for the first few points which suffer from saturation and the region after 50 or 60 arcseconds where the background subtraction is not as effective. In Figure 19 we see the color for NUV – Ch1 and NUV – Ch4. They are again, mostly constant except for the first few and the last few data points. Figure 20 shows NICMOS 1.6 microns – Keck 10.5 microns. Again, the data after 2.5 arcseconds is unreliable due to the small image size. It seems to first get redder for the first 0.5 arcseconds, reaching the reddest value around 0.7 arcseconds and then starts to get bluer. This behavior is actually very similar to the first 3 arcseconds of the STIS FUV-NUV color data in Figure 12. Figure 21 shows that FUV-Keck and NUV-Keck have a similar red dip in the inner 2 arcseconds. It is interesting to note that Worthey (2004) mentions a discontinuity in the light profile of M32 at 2 arcseconds. These color plots confirm this discontinuity as a redder color in the inner 2 arcseconds.

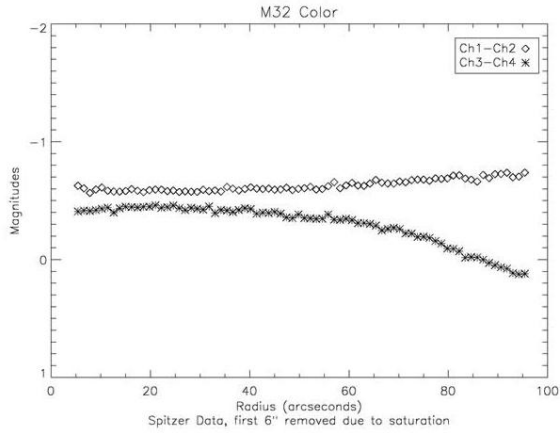


Figure 14: IRAC color data, Channels 1-2 and 3-4

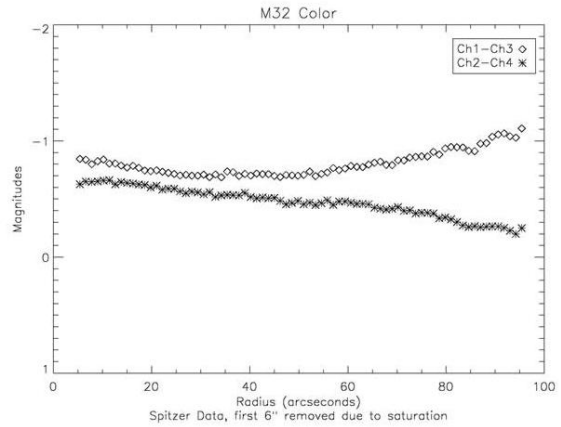


Figure 15: IRAC color data, Channels 1-3 and 2-4

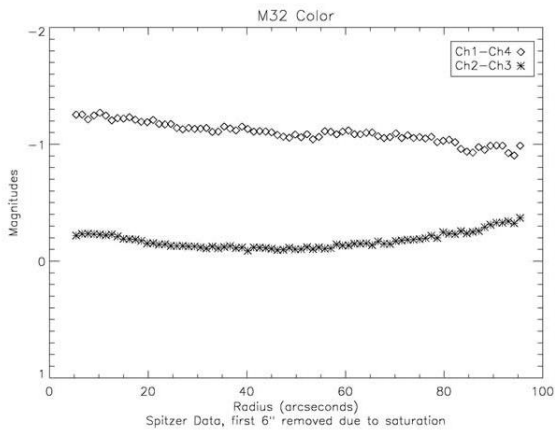


Figure 16: IRAC color data, Channels 1-4 and 2-3

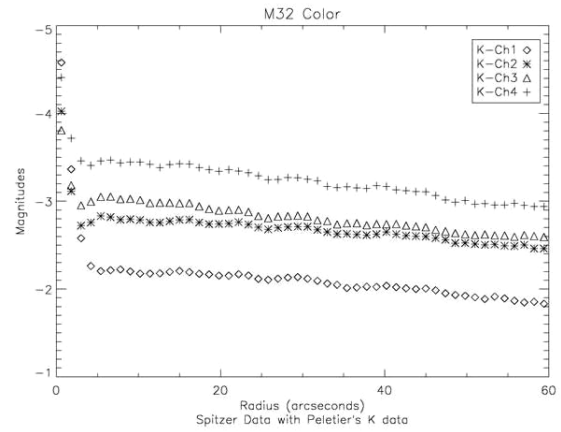


Figure 17: K-IRAC color data

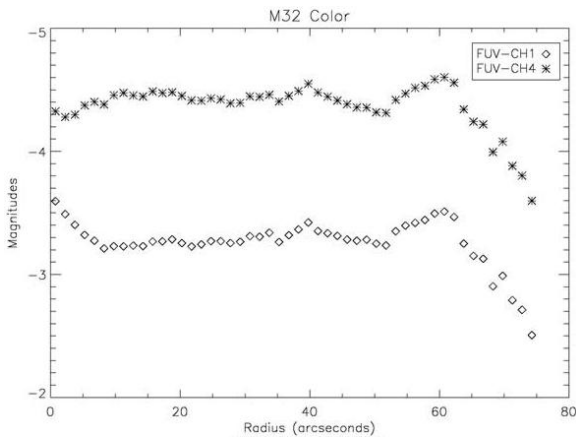


Figure 18: GALEX FUV and IRAC

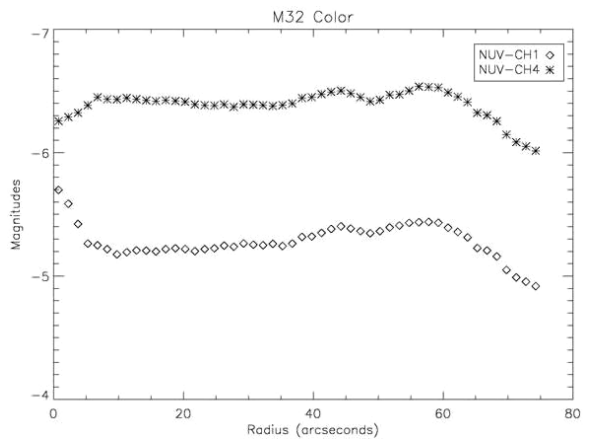


Figure 19: GALEX NUV and IRAC

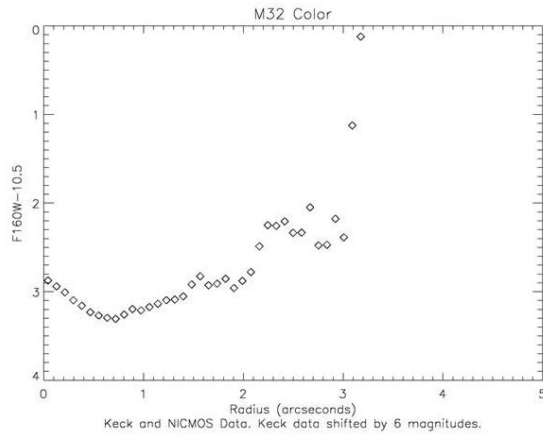


Figure 20: NICMOS and Keck color

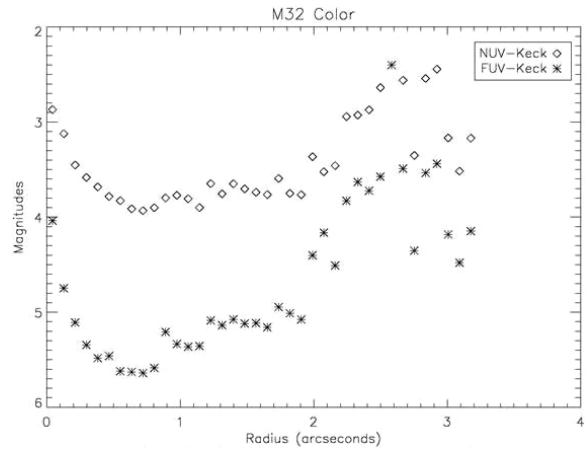


Figure 21: HST STIS and Keck color. FUV-Keck shifted up by 2 magnitudes to be compared with NUV-Keck.

6. Population of Point Sources

Point sources were resolved in the IRAC images. Of special interest is the 8 micron image, since the stars that can be seen at that wavelength are most likely asymptotic branch (AGB) stars. Using the fuel consumption theory, we can determine how long a star will spend in this particular stage and be visible to us at 8 microns. Figure 22 is a histogram plot of the number of stars at a particular luminosity. Although there is some spread in the luminosity, most of the stars lie between -3.5 and -5 magnitudes. Figure 23 shows how the luminosity of stars changes as a function of radius. Figure 24 shows how the number of stars changes as a function of radius. We see more stars near the nucleus than at farther distances. Despite the scatter, we see that it follows a trend similar to that of the surface brightness profile- more numerous at the center and decreasing with distance.

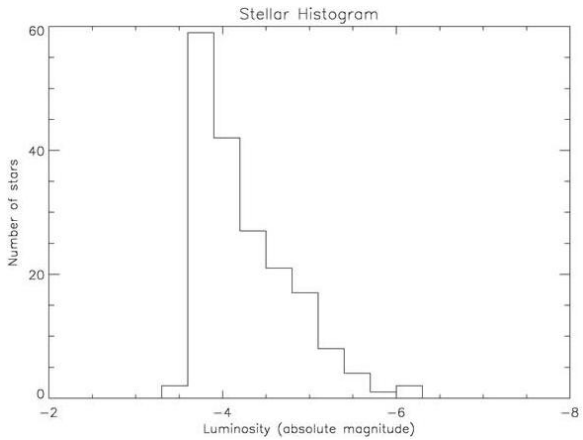


Figure 22: Histogram of stars in IRAC channel 4. Bin size of 0.3 magnitudes.

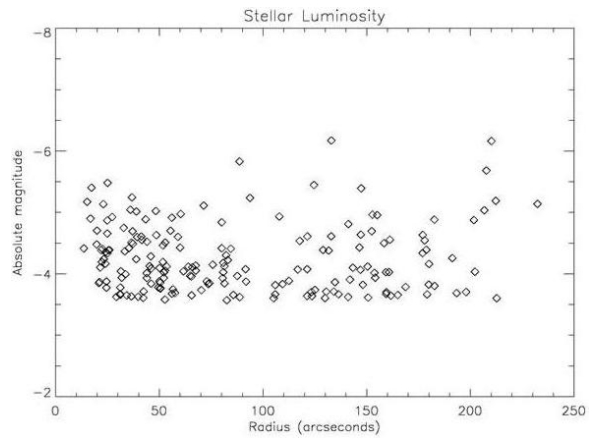


Figure 23: Luminosity of stars vs. radius from galaxy center.

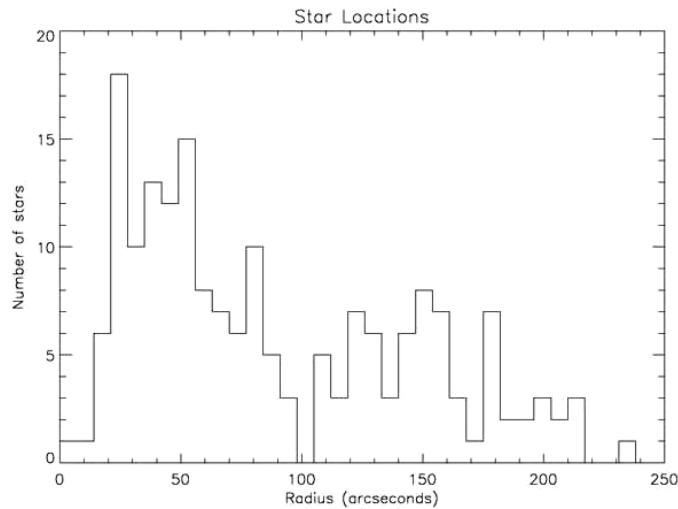


Figure 24: Number of stars vs. radius from center. Bin size is 7 arcseconds.

6.1 Fuel Consumption Theorem

The fuel consumption theorem will give you the number of stars in some stage with a particular lifetime given some luminosity (Renzini and Buzzoni 1986). We know that more luminous stars will burn their fuel faster and evolve through their lives at a faster rate. Given enough time, even the less luminous stars will reach a particular stage in their evolution. We can combine this to get $n = BtL$, where n is the number of stars in the stage we are interested in, t is the lifetime of that stage, L is the luminosity in solar luminosities (L_{\odot}), and B is the rate at which stars leave the main sequence. B is about 2×10^{-11} stars

per year per L_{\odot} (Rich 1998). For these images, we know how many stars there are and we can determine the total luminosity. Thus, we can rewrite the formula as

$$t = \frac{N}{L \cdot 2 \times 10^{-11}}$$

to determine the lifetime of the observed stars.

6.2 Methods

In order to apply the fuel consumption theory we need to determine the number of stars and the total luminosity. We have already determined the number of stars as explained in Section 3.3. There are 183 stars from 14 to 230 arcseconds in the IRAC 8 micron image. For the total luminosity we can integrate the light as observed in Peletier's R data in the region where the stars exist. Unfortunately, the data does not extend out to 230 arcseconds so we take as much as we can and count only the stars that lie within it. The R data extends up to 110 arcseconds and there are 119 stars from 14 to 110 arcseconds. For reference, the Sun has an absolute magnitude of 4.420 in the R band and the distance modulus for M32 is 24.43.

In order to obtain the total luminosity we first measure the magnitude and convert to absolute magnitudes using $M = m - 24.43$. We then convert to solar luminosities by using $L = 10^{\frac{M-4.42}{-2.5}}$. The final step is to multiply by the area of the region to obtain total luminosity.

Two methods were used to integrate the light from the R data. The first method took an average of the R magnitudes within the range where the stars were detected. We converted the magnitude into solar luminosities and used the area of the entire elliptical annulus from 14 to 110 arcseconds. In the second method we take the average of the R magnitudes between two small, concentric ellipses. We convert magnitudes into solar

luminosities and take the area of the small elliptical annulus. We then repeat the process for another small elliptical annulus and add the luminosity of this new region. We repeat this until we have gone through the entire area we wished to measure. The second method provides a more accurate measure of the total luminosity enclosed in the area.

6.3 Results

We obtained two different results for our two methods, yet they differ by less than a factor of 2. Method 1, which used an average magnitude, yielded a total luminosity of $2.2 \times 10^8 L_{\odot}$ and a lifetime of about 27,000 years. Method 2 yielded a total luminosity of $1.4 \times 10^8 L_{\odot}$ and a lifetime of about 44,000 years. They do not vary significantly, so we can say that these stars are in a phase whose lifetime is somewhere around 27 to 44 thousand years. The lifetime of the rapid mass loss phases is not well known, but it is expected to be around 10- 20 thousand years.

7. Interpretation

The color plots are fairly constant with only gradual changes. This leads us to believe that the stellar population is roughly the same throughout the galaxy. The relative lack of a color gradient in FUV-8 μ m is satisfying since we expect helium burning and rapidly mass losing stars to be relatively brief phases of stellar evolution. The gradual slopes are mostly showing a bluer interior. The slopes of some of these images may indicate that certain groups of stars are more common at certain radii than at others. It may also indicate differences in metallicity or age since these could affect the properties of helium burning and mass loss.

The STIS FUV-NUV and NICMOS-Keck color plots are close ups of the first few arcseconds and show an interesting feature. Both have an increasing redder color for the first arcsecond with the reddest value at 0.7 arcseconds, after which it begins to get bluer. For the STIS data, it starts to flatten out after about 3 or 4 arcseconds. This seems to show that there is something within the first few arcseconds that is causing this redder color. The divided image, Figure 13, shows a dark feature that could be dust. This dust, which might come from the AGB stars, could explain the redder color since dust blocks the shorter wavelengths more readily. At the galaxy's distance of 750kpc, 2 arcseconds correspond to about 7 parsecs (nearly 24 light-years). Worthey (2004) also observed a discontinuity in the surface brightness profile of M32 at 2 arcseconds, yet his study of stellar populations using spectra did not reveal the presence of a different population in that region.

Counting point sources and applying the fuel consumption theorem give a lifetime of 27,000 to 44,000 years for the observed stars in IRAC channel 4. This agrees within a factor of four or so to the lifetime of AGB stars.

8. Conclusion

In conclusion, our color plots of M32 show a constant color throughout the galaxy with only gradual changes. This is indicative of the same stellar population at all radii from M32's center. We also see a redder color in the inner 7 parsecs of the galaxy that may be caused by dust.

Our analysis of the point sources in the IRAC 8 micron images showed 119 stars in the region from 14 to 110 arcseconds from the center of M32. These stars are AGB stars whose lifetime was calculated to be somewhere around 27,000 or 44,000 years.

Acknowledgements

We would like to acknowledge Gil de Paz for providing the higher signal to noise ratio GALEX images used in our analysis. We would also like to thank the mentors, Mark Morris and Mike Rich, and the post doc, David Reitzel, for all their help and support. We are grateful to NSF and the UCLA Physics and Astronomy Department for hosting this summer research program.

Appendix A: General Telescope Information

GALEX

The Galaxy Evolution Explorer is a space telescope orbiting at an altitude of about 690 kilometers and an inclination of 29 degrees to the equator. It is a NASA Small Explorer Mission led by the California Institute of Technology. The telescope was successfully launched on April 28, 2003 aboard the Pegasus XL launch vehicle in Cape Canaveral, Florida. It was originally intended as a 29 month mission, but has been recently extended. So far, the GALEX Release 1 (GR1) data is available and GR2 will be available some time after November of 2005. Our data was taken from the GR1 data set, specifically from the Near Galaxy Survey (NGS). After November of 2004, the results of GR1's NGS were available on the MultiMission Archive at the Space Telescope Science Institute (MAST).

The telescope is a 50cm Ritchey-Chrétien telescope with a dichroic beam splitter, which allows the simultaneous imaging of a portion of the sky in both the near and far ultraviolet. Its field of view is about 1.25 degrees in a circular patch of sky. The instrument's resolution, the full width at half max (FWHM) of a point source, is about 4

arcseconds in the far ultraviolet (FUV) and 5.6 arcseconds in the near ultraviolet (NUV). The FUV images use a blue edge filter that centers on a wavelength of 1528 Å and extends from about 1344 to 1786 Å. The near ultraviolet images use a red block filter/fold mirror that allows light from around 1771 to 2831 Å to enter, with a central wavelength of 2271 Å. Data for the GALEX satellite is available on the GALEX², MAST³, and GR1⁴ websites.

Spitzer

The Spitzer Space Telescope, previously known as the Space Infrared Telescope Facility (SIRTF), is the largest infrared telescope that has been launched into space. It was launched on August 25, 2003 by a Delta 7920H rocket from Cape Canaveral. Spitzer is a NASA mission managed by the Jet Propulsion Laboratory. Its mission lifetime was set for only 2.5 years, yet the estimates show that it might last for 5 years.

The telescope is an 85cm cryogenic telescope. Since the telescope observes in the infrared, the cryogenics are required in order to cool the telescope and the instruments to reduce the amount of heat they would contribute to each image. The telescope can observe from 3.6 to 160 microns.

These images were obtained using the Leopard software available on the Spitzer Science Center's website. The images used were taken by the InfraRed Array Camera (IRAC). It is a four channel camera providing images at 3.6, 4.5, 5.8, and 8 microns. Its field of view is about 5.2 by 5.2 arcminutes. Its FWHM is about 1.83" based on point spread functions available on the website. The camera uses a beam splitter so that

² GALEX website available at <http://www.galex.caltech.edu/>

³ MAST GALEX website available at <http://galex.stsci.edu/GR1/>

⁴ GR1 website available at http://www.galex.caltech.edu/DATA/gr1_docs/

channels 1 and 3 (3.6 and 5.8microns, respectively) image one portion of the sky and channels 2 and 4 (4.5 and 8microns, respectively) image an adjacent portion. Channels 1 and 2 use InSb detector arrays operating at ~15K, while channels 3 and 4 use Si:As detectors at ~6K. Data for the Spitzer Space Telescope is available on the Caltech Spitzer website⁵ and Spitzer Science Center (SSC) website⁶.

Keck

The Keck telescopes are the largest optical telescopes on the Earth. They are located on Mauna Kea at almost 14,000 feet in Hawaii. They are two 10-meter telescopes, whose primary mirrors are made from 36 1.8-meter hexagonal pieces. The telescopes can make use of adaptive optics, which deforms a correcting mirror in such a way to correct for atmospheric distortions.

The images we used were taken using the Long Wavelength Spectrometer (LWS). This instrument provides images in the 3-25micron range from the Cassegrain focus on Keck I. It can image a 10.2 by 10.2 arcseconds field of view with its Si:As detector array and has a FWHM of about 0.26 arcseconds. It uses a mode of operation known as chop-nod, which allows you to get dark images in order to subtract some of the background noise in the image. This information is available on the Keck⁷ and LWS⁸ websites.

HST

The Hubble Space Telescope (HST) is an orbiting telescope that operates from the near-infrared to the ultraviolet. It is a 2.4m telescope orbiting the Earth at an altitude of

⁵ Spitzer website available at <http://www.spitzer.caltech.edu/about/index.shtml>

⁶ SSC website available at <http://ssc.spitzer.caltech.edu/geninfo/>

⁷ Keck website available at <http://www2.keck.hawaii.edu/geninfo/about.php>

⁸ LWS website available at <http://www2.keck.hawaii.edu/inst/lws/>

about 600 kilometers. It was launched on April 25, 1990 from the space shuttle Discovery (STS-31). HST is operated by the Space Telescope Science Institute (STScI). Since it is above the atmosphere, it can achieve resolutions down to 0.1 arcseconds. It has been serviced several times by the space shuttle. The HST images were downloaded from the MAST database. This information on HST can be found on the HST⁹ and MAST¹⁰ websites.

HST NICMOS

The Near-Infrared Camera and Multi-Object Spectrometer (NICMOS) is one of the several instruments aboard the HST. NICMOS operates in the 0.8 to 2.5 micron range. It has three cameras that can operate simultaneously. The image we used was taken by the second camera, NIC2, with the F160W filter. The detector is a HgCdTe 256x256 pixel array. The F160W filter allows light from 1.4 to 1.8 microns and is centered at roughly 1.6microns. Data for NICMOS obtained from the online NICMOS handbook¹¹.

HST STIS

The Space Telescope Imaging Spectrograph (STIS) is another instrument aboard the HST. It operates from the ultraviolet to the near-infrared. It has three detectors, the one we used were the Cs₂Te Multi Anode Microchannel Array in near UV (NUV-MAMA) and the CsI FUV-MAMA for the far UV. The filters used were F25QTZ (made of Quartz) for NUV and F25SRF2 (made of SrF₂) for FUV. The F25QTZ filter allows light from 1460 to 3270 Å centered at 2354 Å. The F25SRF2 filter allows light from 1280

⁹ HST website available at http://www.stsci.edu/hst/HST_overview/

¹⁰ MAST HST website available at <http://archive.stsci.edu/hst/>

¹¹ NICMOS handbook available at http://www.stsci.edu/hst/nicmos/documents/handbooks/current_NEW/nicmos_instr_handbookTOC.html

to 1780 Å centered at 1469 Å. These wavelength ranges are comparable to the GALEX FUV and NUV. Since the field of view for STIS is 25 by 25 arcseconds, it serves as a close up image of M32 in the ultraviolet. Data for STIS obtained from the online STIS handbook¹².

Appendix B: Reduction of Keck Data

Here we describe the procedure used to reduce the Keck data. We have a total of six images, three of which have M32 at its center and the other three have it displaced toward the lower right edge. The IDL routine **lwscoadd**, provided on the LWS website, automatically adds and subtracts the necessary frames from the chop-nod cycles to get the best sky subtracted image. These background images obtained from the nodding are necessary, since the surroundings at room temperature (~300K) have a peak wavelength close to 10.5 microns, the wavelength being observed. Even after this, several more steps are made to improve the images. First, three of the images with M32 in the center are added and the other three with M32 off-center are also added yielding two images that are shifted from one another. Then, the bad pixels are removed from both images; one of the images with bad pixels is shown in Figure 25. Pixel removal is done using the IDL routine **sigma_filter** which replaces points that differ by more than a user-specified number of sigma (usually 3-5) from its surroundings by the average value of its surroundings. One of the images had a significant background gradient across it- the image is brighter at the bottom than at the top, as can be seen in Figure 26. This is corrected by subtracting out a plane from that image, obtaining Figure 27. We then shift

¹² STIS handbook available at http://www.stsci.edu/hst/stis/documents/handbooks/currentIHB/stis_ihbTOC.html

one image and added it to the other to obtain a final image that was the sum of all 6 images; this is shown in Figure 28. This image looks much better, yet still had some noise. The final step is convolving the image with a point spread function (PSF) of 3 pixels (0.25 arcseconds), which is the ideal diffraction limit of the telescope at that wavelength. The IDL routines **psf_gaussian** and **convolve** are used to perform this final task. The final convolved image is shown in Figure 29.



Figure 25: Keck image with bad pixels

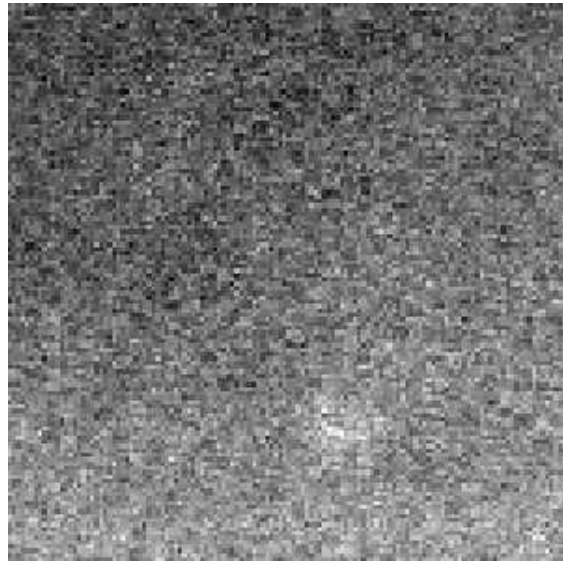


Figure 26: Keck image with bad pixels removed

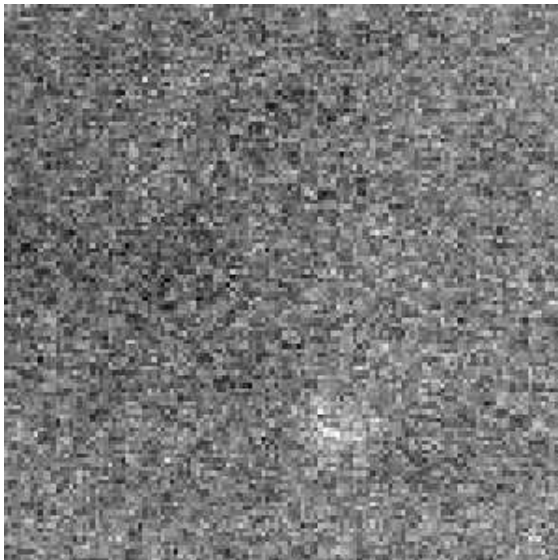


Figure 27: Keck image with gradient subtracted



Figure 28: Sum of all Keck images

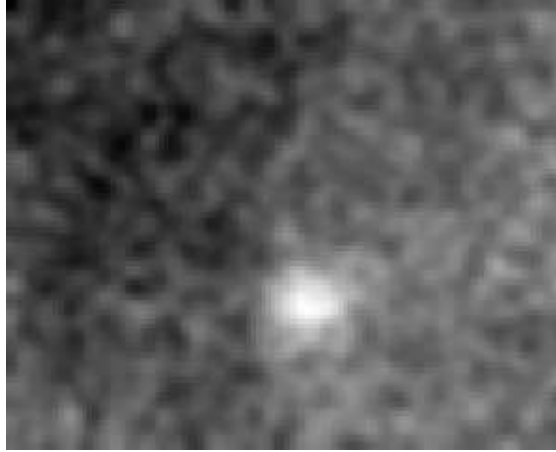


Figure 29: Final convolved Keck image

Appendix C: Regions of Stellar Formation in M31

The Spitzer IRAC images and GALEX images have large fields of view that show features from the nearby Andromeda Galaxy (M31). Figure 30 is the IRAC 8 micron image of M32 and its surroundings. To the right of the image we can see clouds of dust and PAH (Polycyclic Aromatic Hydrocarbon) regions belonging to M31. Figure 31 is a FUV GALEX image that has been rotated and scaled in order to compare it with the IRAC 8 micron image. In the ultraviolet, we can see regions of star formation to the West and Northwest of M32. We superimposed these two images in Figure 32 to show how the regions of star formation compare with the PAH regions, using FUV as blue and 8 microns as orange. The results show that the star forming regions are not in the same location as the PAH regions, and that star formation is actually forming in the darker regions of decreased PAH emission.

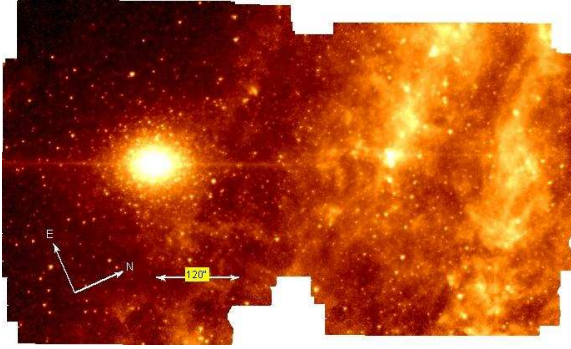


Figure 30: M32 at 8 microns (IRAC)

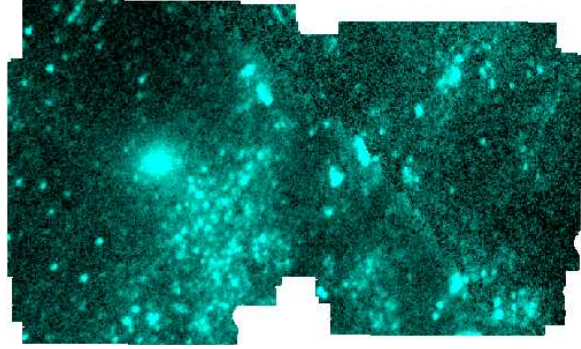


Figure 31: M32 in FUV (GALEX)

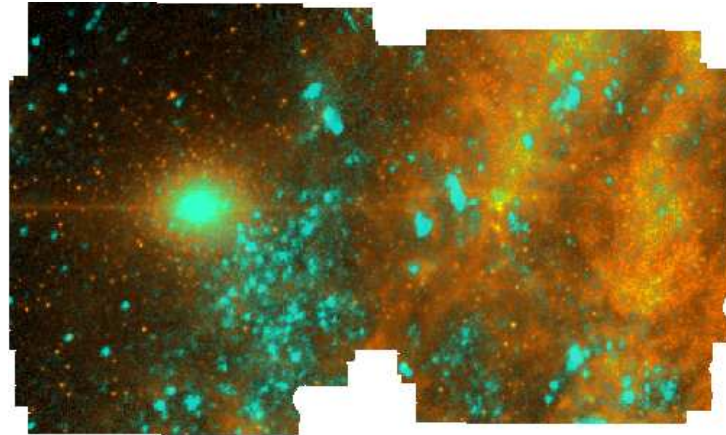


Figure 32: M32 combined image. Blue is FUV; orange is 8 microns.

References

Gil de Paz A., et al., 2003, AAS Meeting 203, 9606

Kormendy J. & Richstone D., 1995, ARAA, 33, 581

Oke J. B., 1990, AJ, 99, 1621

Peletier R. F., 1993, A&A, 271, 51

Renzini A. & Buzzoni A., 1986, in Spectral Evolution of Galaxies, 195

Rich R. Michael, 1998, ASPC, 113, 129

Rose James A., et al., 2005, AJ, 129, 712

Worthey G., 2004, AJ, 128, 2826